Electronic Supplementary Information

Iron carbonate hydroxide templated binary metal-organic frameworks for highly efficient electrochemical water oxidation

Jian Du,[a] Suxian Xu,[a] Licheng Sun[a,b] and Fei Li*,[a]

[a] State Key Laboratory of Fine Chemicals, DUT-KTH Joint Education and Research Center on Molecular Devices, Dalian University of Technology, Dalian, 116024, China

[b] Department of Chemistry School of Engineering Sciences in Chemistry, Biotechnology and Health KTH Royal Institute of Technology, Stockholm, 10044, Sweden

E-mail: lifei@dlut.edu.cn

Experimental section

Materials

All chemicals and solvents were commercially available and used without further purification. Iron nitrate nonahydrate ($Fe(NO_3)_3·9H_2O$, 99.99%), Iron chloride hexahydrate ($FeCl_3·6H_2O$, 99%), Urea ($Co(NH_2)_2$, 99%), Ammonium fluoride (NH_4F, 98%), Terephthalic acid ($C_8H_6O_4$, 99%) and potassium hydroxide (KOH, 95%) were purchased from Aladdin chemical company. Ethanol (C_2H_5OH) and N, N-dimethylformamide (DMF) were analytical pure and purchased from commercial supplier. Ni foam (1cm × 2cm, thickness: 1.5 mm, bulk density: 2000 mg cm^{-3}) were purchased from Suzhou jiashide metal foam Co.,ltd.

Fabrication of FeCH-NF, NiFe-MOF/FeCH-NF and Ni-MOF-NF electrodes

Ni foam (NF, 1cm × 2cm) was firstly immersed in 1M HCl solution for 30 minutes to remove surface oxides and pollutants. Iron carbonate hydroxide (FeCH) was coated on NF by hydrothermal synthesis according to a modified literature procedure.[1] Generally, 2 mmol $Fe(NO_3)_3·9H_2O$ (808 mg), 20 mmol $CO(NH_2)_2$ (1200 mg) and 1 mmol NH_4F (37 mg) were dissolved in 30 ml water and stirred to form a clear solution. The obtained solution together with acid treated NF were then sealed in a 50 ml Teflon-lined stainless steel autoclave and heated at 120 ℃ for 8 h. After washing with ethanol and deionized water for several times, the as-prepared FeCH-NF was transferred into another 50 mL Teflon-lined stainless steel autoclave containing terephthalic acid (30 mg) and DMF/ethanol/water (3 mL/10 mL /10 mL). After maintaining at 120 ℃ for 6 h, the resultant NiFe-MOF/FeCH-NF electrode was rinsed with deionized water and dried at 60 ℃ to get the target NiFe-MOF/FeCH-NF. Ni-MOF-NF electrode was prepared as described above except no FeCH coating was made.

Fabrication of NiFe-MOF-NF (0.25), NiFe-MOF-NF (0.5) and NiFe-MOF-NF (0.75) electrodes

NiFe-MOF-NF electrodes were fabricated as described above except extra Fe^{3+} ions were added. Generally, acid treated NF substrates were immersed in the mixed DMF/ethanol/water (3 mL/10 mL/10 mL) solution containing terephthalic acid (30 mg, 0.18 mmol) and $FeCl_3 \cdot 6H_2O$ with various amount of 12.25 mg (0.045 mmol), 24.5 mg (0.09 mmol) and 36.75 mg (0.135 mmol), respectively. The obtained solution together with NF were then sealed in a 50 mL Teflon-lined stainless steel autoclave and heated at 120 ℃ for 6 h. After rinsing with deionized water and ethanol several times, the obtained electrodes were denoted as NiFe-MOF-NF (0.25), NiFe-MOF-NF (0.5) and NiFe-MOF-NF (0.75), respectively.

Fabrication of RuO_2-NF electrode

The RuO_2-NF electrode was prepared by dispersing 5 mg RuO_2 into 1 mL mixed solution containing 0.45 mL ethanol, 0.5 mL water and 0.05 mL 5% Nafion, the mixture was then ultrasonicated for 30 min to become homogenous. Subsequently, 0.15 mL of the suspension was dropped on the NF and dried at 60 ℃ to obtain RuO_2-NF as working electrode.

Material characterization

The morphologies of the as-prepared samples were investigated by Nova NanoSEM 450 equipment. The microstructure was characterized by TEM (FEI TF30). The phase purity and crystallinity were examined by X-ray diffraction (XRD) patterns, which were acquired on a D/max-2400 diffractometer (Japan Rigaku Rotaflex) with Cu Kα radiation ($\lambda = 154.1$ Å). The chemical composition and element states of the samples were analyzed by X-ray photoelectron spectroscopy (XPS) (Thermo Scientific ESCALAB250). The binding energy (BE) was calibrated with respect to the C 1s peak at 284.6 eV. FTIR spectra were conducted on a Thermo Fisher 6700 FT-IR spectrometer with the sample pelleted using KBr powders. Raman spectroscopy were collected on a DXR Smart Raman using Ar^+ laser excitation. The quantitative analysis of metal elements was performed with Inductively Plasma-Atomic Emission (ICP-AES) spectrometer (Optima 2000DV, American PerkinElmer Corp.).

Electrochemical measurements

All the electrochemical measurements were carried out in a three-electrode system on CHI 660E Electrochemical Analyzer (Shanghai Chenhua Instrument Co., LTD) at room temperature in 1 M KOH aqueous solution. A piece of NF (1cm × 2cm) decorated with MOF materials was employed as the working electrode, Pt mesh and HgO/Hg electrode were used as the counter and reference electrodes, respectively. All potentials reported here were converted to the reversible hydrogen electrode (RHE) scale with the equation of $E_{RHE} = E_{HgO/Hg} + 0.0592\ pH + 0.114\ V$.

Before electrochemical tests, the working electrode was activated by a chronoamerometry scan until a stable current obtained (~5 mins). Liner sweep voltammetry (LSV) curves with a scan rate of 5 mV s^{-1} were manually corrected to compensate for the resistance of the electrolyte. Tafel slopes were determined by steady-state current density method and were calculated by plotting overpotential against Log (current density). Chronopotentiometry measurement was carried out under a constant current density of 10 mA cm^{-2} to evaluate the durability. The electrochemical impedance spectroscopy (EIS) was recorded at an overpotential of 250 mV at the amplitude of the sinusoidal voltage of 5 mV over a frequency range from 0.1 Hz to 10^5 Hz. The electrochemical active surface area (ECSA) was estimated by calculating the double-layer capacitance (C_{dl}) from cyclic voltammetry tests at different scan rates (20 to 120 mV s^{-1} with an interval of 20 mV s^{-1}) in a non-faradaic region (0.2-0.3 V vs. HgO/Hg). The value of C_{dl} was determined from the liner plot between current density difference (j_a-j_c) and scan rates, which equals to half of the slope.

Reference

(1) Hui. L, Jia. D, Yu. H, Xue. Y, Li. Y. Ultrathin Graphdiyne-Wrapped Iron Carbonate Hydroxide Nanosheets toward Efficient Water Splitting. *ACS Appl. Mater. Interfaces*, 2019, **11**, 2618.

Additional Experimental Results

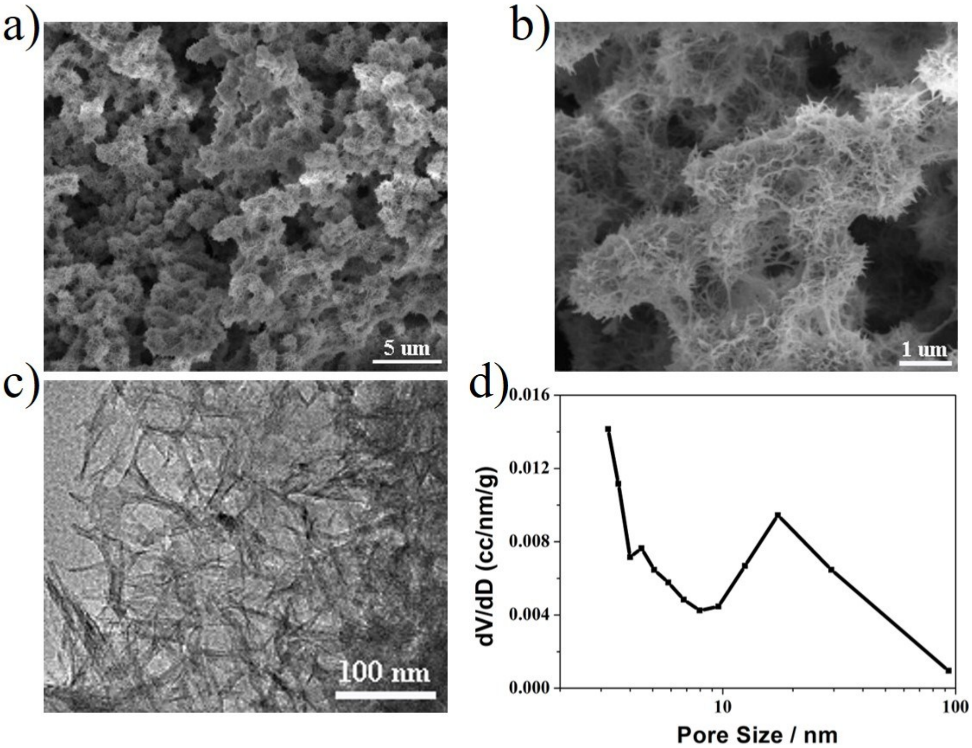

Figure S1. (a-b) SEM images of FeCH-NF under different magnifications; (c) TEM image and (d) pore size distribution curve of FeCH NS.

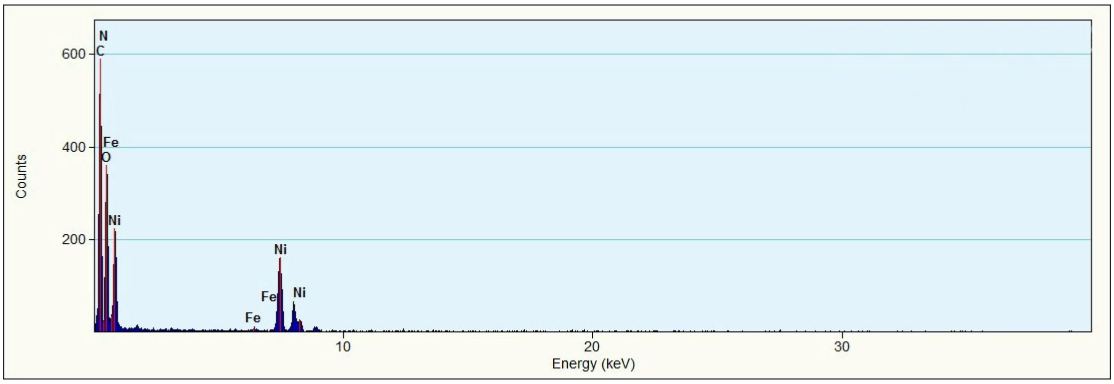

Figure S2. EDX analysis of the as-prepared NiFe-MOF/FeCH-NF.

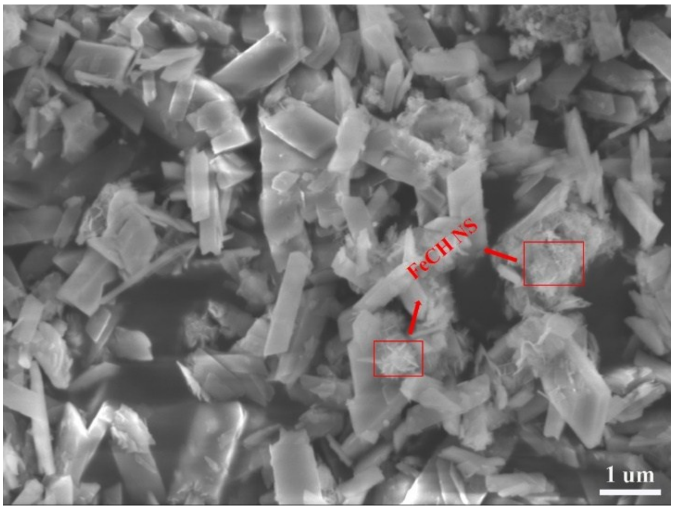

Figure S3. SEM images of NiFe-MOF/FeCH powder scraped from NF substrate. The red framed region indicates the co-existence of FeCH nanosheets and NiFe-MOF nanoplates.

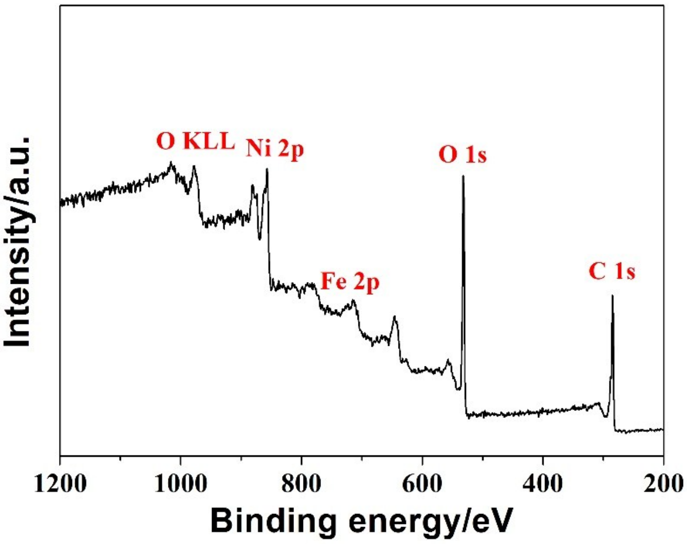

Figure S4. XPS survey spectrum of NiFe-MOF/FeCH-NF.

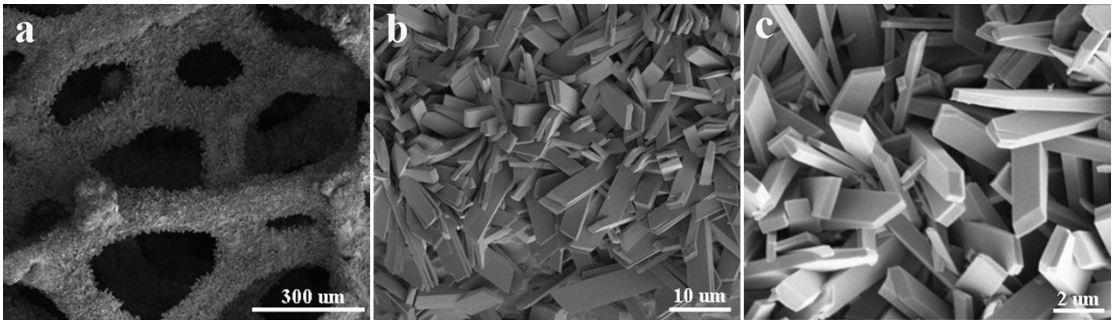

Figure S5. (a-c) SEM images of Ni-MOF-NF under different magnifications.

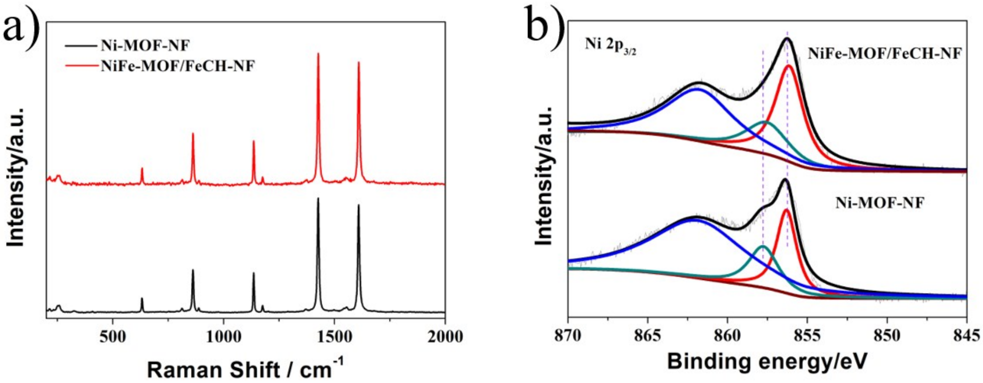

Figure S6. (a) Raman spectra and (b) Ni 2p$_{3/2}$ XPS core level spectra of Ni-MOF-NF and NiFe-MOF/FeCH-NF.

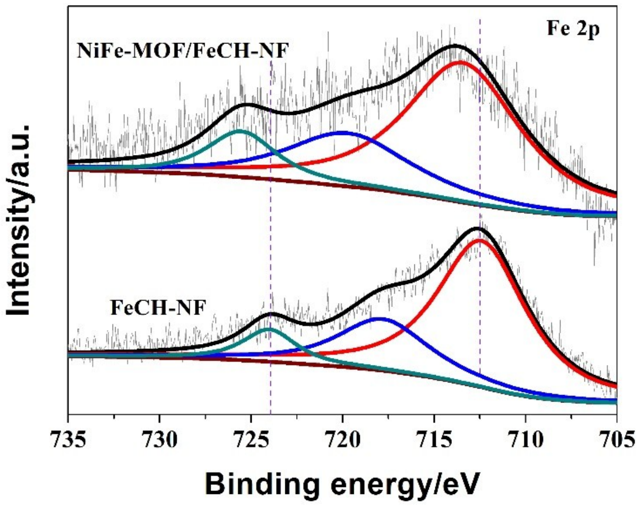

Figure S7. High-resolution XPS spectra of Fe 2p for FeCH-NF and NiFe-MOF/FeCH-NF.

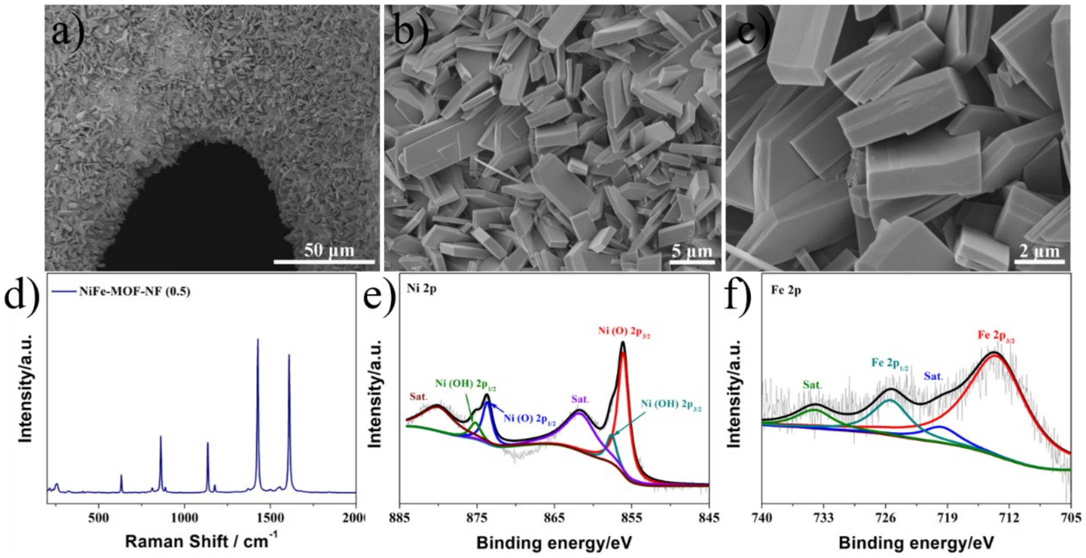

Figure S8. (a-c) SEM images of NiFe-MOF-NF (0.5) under different magnifications; (b) Raman spectrum of NiFe-MOF-NF (0.5); High-resolution XPS spectra of (c) Ni 2p and (d) Fe 2p for NiFe-MOF-NF (0.5). The Ni $2p_{3/2}$ and Ni $2p_{1/2}$ peaks at the binding energy of 856.1 and 873.68 eV are attributed to the coordination bonds between Ni and carboxylate oxygen. The others at 857.6 and 875.2 eV can be assigned to the Ni-OH corresponding to the links between Ni^{2+} and hydroxyl group. The Fe $2p_{3/2}$ and Fe $2p_{1/2}$

peaks at the binding energy of 713.4 and 725.4 eV confirm the existence of Fe^{3+}. The chemical states for both Ni and Fe were almost the same as those in NiFe-MOF/FeCH-NF, indicating the formation of NiFe-MOF-NF (0.5) electrode.

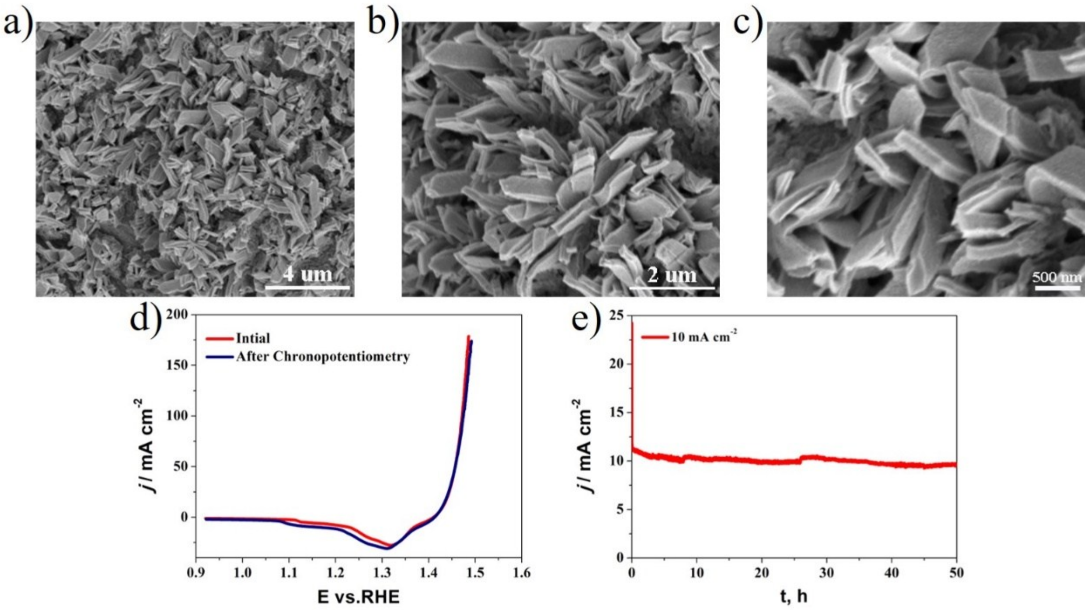

Figure S9. (a-c) SEM images of NiFe-MOF/FeCH-NF after long-term durability test; (d) LSV curves of NiFe-MOF/FeCH-NF before and after chronopotentiometric measurement; (e) Chronoamperometric measurement of NiFe-MOF/FeCH-NF at 1.45 V.

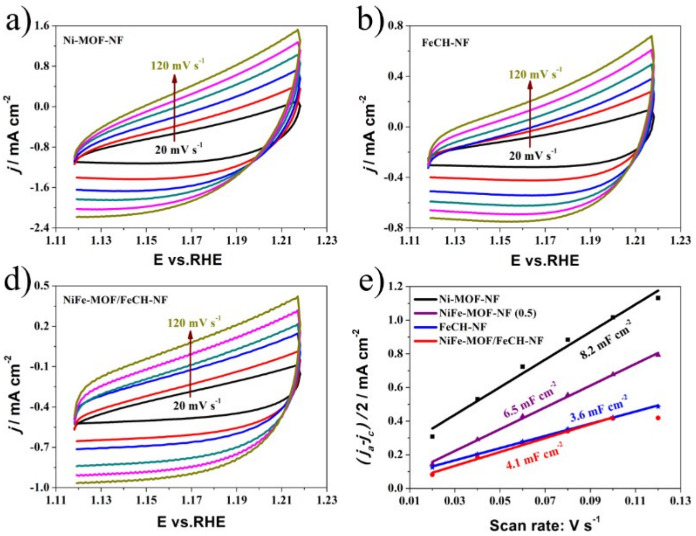

Figure S10. CV curves of (a) Ni-MOF-NF, (b) FeCH-NF, (c) NiFe-MOF-NF (0.5) and (d) NiFe-MOF/FeCH-NF at various scan rates (20 to120 mV s^{-1} with an interval of 20 mV s^{-1}) within the potential range of 1.12~1.22 V; (e) Charging current density difference at 1.17 V plotted against scan rate for Ni-MOF-NF, NiFe-MOF-NF (0.5), FeCH-NF and NiFe-MOF/FeCH-NF.

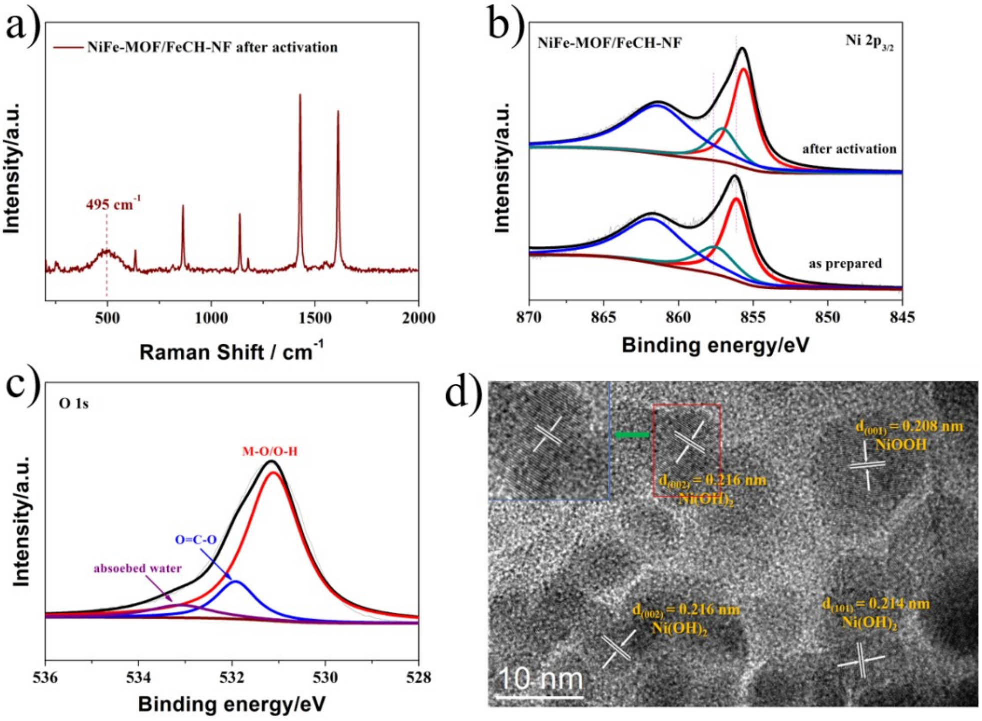

Figure S11. (a) Raman spectrum of NiFe-MOF/FeCH-NF after activation treatment; (b) Ni 2p$_{3/2}$ XPS core level spectra of NiFe-MOF/FeCH-NF before and after activation. (c) High-resolution O 1s XPS spectrum and (d) TEM image of NiFe-MOF/FeCH-NF after activation.

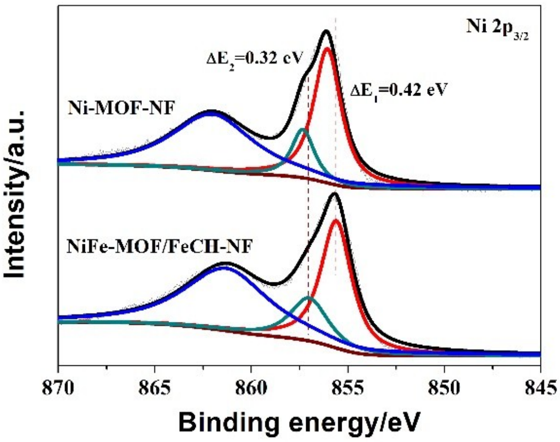

Figure S12. High-resolution XPS spectra of Ni 2p$_{3/2}$ for activated Ni-MOF-NF and NiFe-MOF/FeCH-NF electrodes.

Table S1. OER performance of NiFe-MOF/FeCH-NF and the recently reported NiFe MOF-based electrocatalysts.

Electrocatalyst	Electrolyte	η_{10}/ mV	Tafel slope: mV/dec	References
NiFe-MOF/FeCH-NF	**1M KOH**	**200**	**51.3**	**This work**
NH_2-MIL-88B(Fe_2Ni)/NF	1M KOH	240	58.8	Adv. Energy Mater 2018, 1801065
NiFe-MOF-74/NF	1M KOH	223	71.6	Chem. Commun. 2018, 54, 7046
NiFe-NFF	1M KOH	227	38.9	Adv. Funct. Mater 2019, 29, 1807418
Ni-MOF@Fe-MOF/GC	1M KOH	265	82	Adv. Funct. Mater 2018, 28, 1801554
Fe_1Ni_2-BDC/GC	1M KOH	260	35	ACS Energy Lett. 2019, 4, 285
NF-PBA/GC	1M KOH	258	46	J. Am. Chem. Soc. 2018, 140, 11286
Fe/$Ni_{2.4}$-MIL-53/GC	1M KOH	244	48.7	Angew. Chem. Int. Ed. 2017, 57, 1888
Ni-Fe-UMNs/GC	1M KOH	260	30	Nano Energy 2018, 44, 345